

Downloaded from UvA-DARE, the institutional repository of the University of Amsterdam (UvA)
<http://hdl.handle.net/11245/2.30142>

File ID uvapub:30142
Filename 135877y.pdf
Version unknown

SOURCE (OR PART OF THE FOLLOWING SOURCE):

Type article
Title Hole distribution for (Sr,Ca,Y,La)₁₄Cu₂₄O₄₁ ladder compounds studied by x-ray absorption spectroscopy
Author(s) N. Nücker, M. Merz, C.A. Kuntscher, S. Gerhold, S. Schuppler, R. Neudert, M.S. Golden, J. Fink, D. Schild
Faculty UvA: Universiteitsbibliotheek
Year 2000

FULL BIBLIOGRAPHIC DETAILS:

<http://hdl.handle.net/11245/1.423963>

Copyright

It is not permitted to download or to forward/distribute the text or part of it without the consent of the author(s) and/or copyright holder(s), other than for strictly personal, individual use, unless the work is under an open content licence (like Creative Commons).

Hole distribution in $(\text{Sr,Ca,Y,La})_{14}\text{Cu}_{24}\text{O}_{41}$ ladder compounds studied by x-ray absorption spectroscopy

N. Nücker, M. Merz, C. A. Kuntscher, S. Gerhold, and S. Schuppler
Forschungszentrum Karlsruhe, IFP, P.O. Box 3640, D-76021 Karlsruhe, Germany

R. Neudert,* M. S. Golden, and J. Fink
Institut für Festkörper- und Werkstofforschung Dresden, P.O. Box 270016, D-01171 Dresden, Germany

D. Schild
Forschungszentrum Karlsruhe, INE, P.O. Box 3640, D-76021 Karlsruhe, Germany

S. Stadler, V. Chakarian, J. Freeland,† and Y. U. Idzerda
Naval Research Laboratory, Code 6345, Washington, DC 20375

K. Conder
Laboratorium für Festkörperphysik, ETH Zürich, CH-8093 Zürich, Switzerland

M. Uehara, T. Nagata, J. Goto, and J. Akimitsu
Department of Physics, Aoyama-Gakuin University, Chitosedai, Setagaya-ku, Tokyo 157-8572, Japan

N. Motoyama, H. Eisaki, and S. Uchida
Department of Superconductivity, The University of Tokyo, Bunkyo-ku, Tokyo 113-0033, Japan

U. Ammerahl
*Laboratoire de Physico-Chimie des Solides, Université de Paris-Sud, F-91405 Orsay Cedex, France
and II. Physikalisches Institut, Universität zu Köln, Zùlpicher Str. 77, D-50937 Köln, Germany*

A. Revcolevschi
*Laboratoire de Physico-Chimie des Solides, Université de Paris-Sud, F-91405 Orsay Cedex, France
(Received 18 February 2000)*

The unoccupied electronic structure for the $\text{Sr}_{14}\text{Cu}_{24}\text{O}_{41}$ family of two-leg ladder compounds was investigated for different partial substitutions of Sr^{2+} by Ca^{2+} , leaving the nominal hole count constant, and by Y^{3+} or La^{3+} , reducing the nominal hole count from its full value of 6 per formula unit. Using polarization-dependent x-ray absorption spectroscopy on single crystals, hole states on both the chain and ladder sites could be studied. While for intermediate hole counts all holes reside on O sites of the chains, a partial hole occupation on the ladder sites in orbitals oriented along the legs is observed for the fully doped compound $\text{Sr}_{14}\text{Cu}_{24}\text{O}_{41}$. On substitution of Ca for Sr orbitals within the ladder planes but perpendicular to the legs receive some hole occupation as well.

I. INTRODUCTION

Spin-1/2 Heisenberg ladder compounds have been the subject of extensive investigations over the last few years,¹ first and foremost due to their magnetic peculiarities. These are caused by the magnetic interactions within the legs and the rungs which, in principle, may be very different for the various sublattice units. Assuming, e.g., a coupling across the rungs that is much larger than that along the legs leads to the formation of a spin gap for compounds with even numbers of legs and to a tendency for “hole pairing.” Both features turn out to persist even for fairly similar coupling constants as in fact found for many actual ladder compounds. Early on, superconductivity was predicted for even-leg ladders² and was eventually found for $\text{Sr}_{0.4}\text{Ca}_{13.6}\text{Cu}_{24}\text{O}_{41.8}$.³ This compound is a member of the more complex family

$(\text{Sr,Ca})_{14}(\text{CuO}_2)_{10}(\text{Cu}_2\text{O}_3)_7$, which contains layers of Cu_2O_3 two-leg ladders extending along the crystallographic c axis (see Fig. 1); the ladder layers are stacked along the b axis and alternate with layers of edge-sharing CuO_2 chains.^{4,5} The observation of superconductivity is highly remarkable as this compound is a cuprate but does not contain the CuO_2 planes so characteristic for high-temperature superconductors (HTSC’s). It is, therefore, not surprising that these findings initiated a flurry of experimental and theoretical investigations on these compounds, their electronic structure, and its relationship to the magnetic properties.

According to its composition, $\text{Sr}_{14}\text{Cu}_{24}\text{O}_{41}$ is doped by six holes per formula unit (f.u.), which are generally believed to reside essentially in the chain. Perhaps the simplest indication for this is provided by bond-valence-sum (BVS) calculations,⁶ giving higher BVS values for holes in the

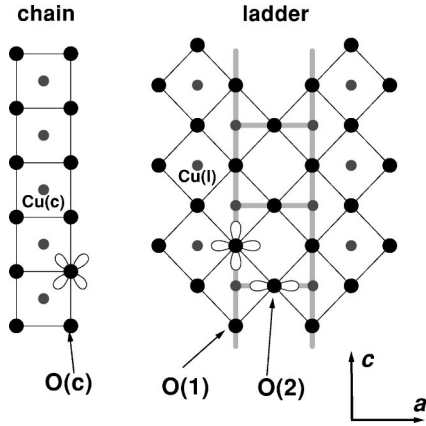


FIG. 1. Structural elements of $\text{Sr}_{14}\text{Cu}_{24}\text{O}_{41}$. Shown are chain units consisting of $\text{Cu}(c)$ and $\text{O}(c)$ sites, and ladder units consisting of $\text{Cu}(l)$ and $\text{O}(1,2)$ sites, with the ‘‘legs’’ and ‘‘rungs’’ highlighted for one ladder as shaded lines. The chain and ladder layers are stacked alternately along the b axis, with Sr sites in between, to form the actual crystal structure.

chains. Similar to the HTSC’s, the holes are expected to be mainly of O $2p$ character as the large Hubbard correlation energy for Cu $3d$ states prevents them from having much Cu character. On the experimental side, resistivity and magnetic measurements on ‘‘undoped’’ $\text{La}_6\text{Ca}_8\text{Cu}_{24}\text{O}_{41}$, with purely a Cu^{2+} valence and thus no holes, as well as on compounds with increasing Sr content for La and a corresponding number of doped holes led to the conclusion that *all* doped holes reside on the chains of $\text{Sr}_{14}\text{Cu}_{24}\text{O}_{41}$, giving a $\text{Cu}^{2.6+}$ valence there.⁷ Neutron scattering,^{9,10} however, points to a spin dimerization along the chain, which in turn was interpreted as a signature for a charge-density-wave- (CDW-) like arrangement of one hole for every other $\text{Cu}(c)$ site of the chain. This means that in total only five out of the six doped holes reside in the $(\text{CuO}_2)_{10}$ chain subunit of $\text{Sr}_{14}\text{Cu}_{24}\text{O}_{41}$, leaving one hole for the $(\text{Cu}_2\text{O}_3)_7$ ladder unit. Optical investigations^{11,12} are also consistent with a hole count of 1 in the ladder unit of $\text{Sr}_{14}\text{Cu}_{24}\text{O}_{41}$; upon Ca substitution this was found to increase to up to 2.8 holes. A recent Cu NMR study¹³ relates measured spin correlation lengths to the average distance between holes and determines a hole occupation on the ladder sites up to 1.75 holes for $\text{Sr}_{2.5}\text{Ca}_{11.5}\text{Cu}_{24}\text{O}_{41}$. The formation of dimers was supported by further NMR (Ref. 14) and nuclear quadrupole resonance¹⁵ (NQR) experiments, and the corresponding charge ordering was observed by x-ray diffraction.¹⁶ Also, NMR measurements¹⁷ suggest that the spin gap of the ladder unit decreases continuously over the whole substitutional range from zero holes to the fully doped and heavily Ca-substituted compounds until it almost reaches zero, while the spin gap of the chain remains essentially constant, lending support to the notion that it is indeed the ladders that carry the superconductivity. On the other hand, other NMR (Ref. 13) and neutron scattering¹⁸ experiments find a constant spin gap upon Ca substitution for the ladders as well. Chemical pressure by Ca substitution for Sr as well as physical pressure reduces the interlayer distances¹⁹ and increases the twisting of the CuO_2 chain.²⁰ As a consequence, about 30–50 % of the $\text{O}(c)$ atoms reduce their distance to the nearest $\text{Cu}(l)$ atom to a value comparable with the typical $\text{Cu-O}_{\text{apex}}$ distance for HTSC’s.²⁰ A

TABLE I. Overview over all single-crystalline samples $(\text{Sr,Ca,Y,La})_{14}\text{Cu}_{24}\text{O}_{41}$ investigated in the present work. Given is the group providing the crystal, the nominal hole count n_h per formula unit, and the actual deviation from it as determined by volumetry (see text) and expressed as an oxygen content $41 + \delta$.

Nominal composition	Group	n_h	δ
$\text{La}_6\text{Ca}_8\text{Cu}_{24}\text{O}_{41}$	U Tokyo (2)	0	0.42; 0.43
$\text{La}_5\text{Ca}_9\text{Cu}_{24}\text{O}_{41}$	U Paris	1	0.14
$\text{La}_3\text{Sr}_3\text{Ca}_8\text{Cu}_{24}\text{O}_{41}$	U Tokyo	3	0.02
$\text{Y}_3\text{Sr}_{11}\text{Cu}_{24}\text{O}_{41}$	AGU Tokyo	3	0.05
$\text{La}_2\text{Ca}_{12}\text{Cu}_{24}\text{O}_{41}$	U Paris	4	–
$\text{Sr}_{14}\text{Cu}_{24}\text{O}_{41}$	AGU Tokyo; U Paris	6	0.00; -0.02
$\text{Sr}_9\text{Ca}_5\text{Cu}_{24}\text{O}_{41}$	U Paris	6	–
$\text{Sr}_5\text{Ca}_9\text{Cu}_{24}\text{O}_{41}$	U Paris	6	-0.08
$\text{Sr}_{2.5}\text{Ca}_{11.5}\text{Cu}_{24}\text{O}_{41}$	AGU Tokyo	6	-0.07
$\text{Sr}_2\text{Ca}_{12}\text{Cu}_{24}\text{O}_{41}$	U Paris	6	–

transfer of holes from the chains to the ladder sites concurrent with Ca substitution was predicted theoretically²¹ and was also inferred from various experiments.^{11,12,22}

Despite all this wealth of information on the ladder compounds, however, there remains a considerable amount of controversy, and a more *direct* determination of the site-specific hole distribution is still missing. Both the evolution of hole distributions with increasing number of holes and with increasing Ca content with its structural implications are important to know. In the present study, polarization-dependent x-ray absorption spectroscopy is applied, which is a proven method to obtain such information. The results, in turn, may help to better understand the electronic structure and possibly the onset of the insulator-metal transition as well as the appearance of superconductivity in these systems.

II. EXPERIMENT AND RESULTS

Single-crystalline samples (typically about 60 mm³ in size) were cut from several cm long crystals grown by the traveling solvent floating zone (TSFZ) method;^{23,24} their compositions are shown in Table I. The formal valence of Cu in the samples was determined by a precision volumetric method²⁵ where an overall accuracy of $<5 \times 10^{-4}$ can be achieved. An average Cu valence $+2 + \varepsilon$ obtained in this way gives a total hole count $n_{\text{Cu}} = 24\varepsilon$, and any deviation from the nominal number of holes expected from stoichiometry, n_h , is accounted for by simply taking the O content, which could not be determined independently, as $41 + \delta$ atoms per formula unit with $\delta = (n_{\text{Cu}} - n_h)/2$. The largest δ observed in the present study occurred for the $\text{La}_6\text{Ca}_8\text{Cu}_{24}\text{O}_{41.43}$ samples and corresponds to 0.86 extra holes. Our investigation by scanning electron microscopy (SEM) and microspot Auger analysis revealed that a few percent of La in these samples is segregated as La-rich precipitates, illustrating the fact that a high La content leads to phase instability in these compounds.²⁴ The $\delta = 0.14$ found for $\text{La}_5\text{Ca}_9\text{Cu}_{24}\text{O}_{41.14}$ may result from the same effect. For none of the other compositions traces of such phases could be detected by SEM or x-ray diffraction; also, much smaller values for δ were observed (Table I).

Polarization-dependent near-edge x-ray absorption fine

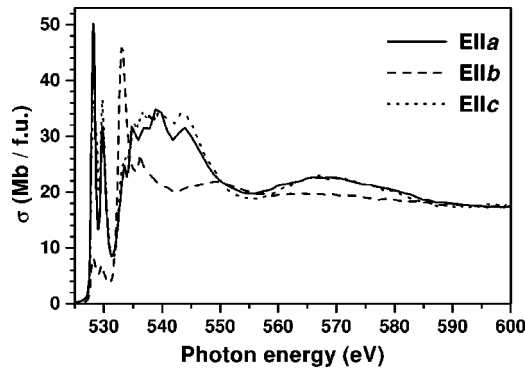


FIG. 2. Polarization-dependent O 1s absorption spectra for $\text{Sr}_{14}\text{Cu}_{24}\text{O}_{41}$. For $\mathbf{E}\parallel a, c$ two large pre-peaks appear below the main absorption edge at about 535 eV; for $\mathbf{E}\parallel b$ these prepeaks are far smaller and a dominant, Sr-related structure appears at the main absorption edge.

structure (NEXAFS) measurements were performed at the National Synchrotron Light Source (NSLS) at the NRL/NSLS beam line U4B. The energy resolution in the range of the O 1s NEXAFS was set to 210 meV. To ensure a flat and shiny surface, several slices (≈ 200 nm each) were cut off from the samples using the diamond blade of an ultramicrotome, and the samples were then transferred to ultrahigh vacuum. The data were recorded at room temperature and in fluorescence detection mode, probing a depth of about 100 nm. The spectra were corrected for incident flux variations and for self-absorption effects,²⁶ and were normalized to tabulated cross sections²⁷ at about 70 eV above the edge where the absorption is atomiclike and structureless. For energy calibration of the O 1s spectra, total electron yield data of NiO were taken simultaneously and referred to a NiO standard²⁸ from electron energy-loss spectroscopy with a reproducibility significantly better than the experimental energy resolution.

The aim of this experiment is to investigate the hole dis-

tribution in the three inequivalent O sites of $(\text{Sr}, \text{Ca}, \text{Y}, \text{La})_{14}\text{Cu}_{24}\text{O}_{41}$. With each of the inequivalent sites, a different Cu-O bond configuration is associated (cf. Fig. 1): a Cu-O-Cu interaction geometry with about 90° for the O(c) sites of the chains, similar to the situation in Li_2CuO_2 ;^{29,30} straight bonds (180°) connecting the Cu(l) sites in the two legs of a single ladder via the rung O(2) sites; and the situation for the O(1) sites of the legs, which form bonds to each of the three neighboring Cu(l) atoms. Assuming that, analogous to the situation in HTSC's, only σ bonds formed between Cu 3d and O 2p states contribute spectral weight near the Fermi level, E_F , there are only five inequivalent O 2p orbitals in the a, c plane (see Fig. 1) which may contribute spectral weight in O 1s NEXAFS. The excitation process in NEXAFS involves the highly localized O 1s core level; moreover, dipole selection rules apply. As a consequence, orienting the electric field vector of the incident radiation, \mathbf{E} , parallel to the crystallographic axes allows one to investigate *specifically* the O 2p orbitals oriented likewise, and thus gain site-specific information on the hole distribution.

Figure 2 depicts the O 1s absorption and its polarization dependence over the full measured energy range for $\text{Sr}_{14}\text{Cu}_{24}\text{O}_{41}$ as a representative example for the whole set of compositions. The two large peaks observed near threshold for the in-plane, $\mathbf{E}\parallel a, c$ spectra are due to Cu-O hybridization and are strongly suppressed for the out-of-plane, $\mathbf{E}\parallel b$ spectrum. The latter exhibits right at the main absorption edge a strong feature which is most likely associated with Sr-O hybrids connecting the chain and ladder layers. In the extended (EXAFS) range the variation of the absorption coefficient σ is very different from that for the in-plane geometry, illustrating that the spatial environment of O in the direction perpendicular to the planes is very different from that within the planes.

O 1s NEXAFS spectra for $(\text{Sr}, \text{Ca}, \text{Y}, \text{La})_{14}\text{Cu}_{24}\text{O}_{41}$ are shown in Fig. 3 for all three orientations $\mathbf{E}\parallel a$, $\mathbf{E}\parallel b$, and $\mathbf{E}\parallel c$ in the energy range of interest below the main edge. Concen-

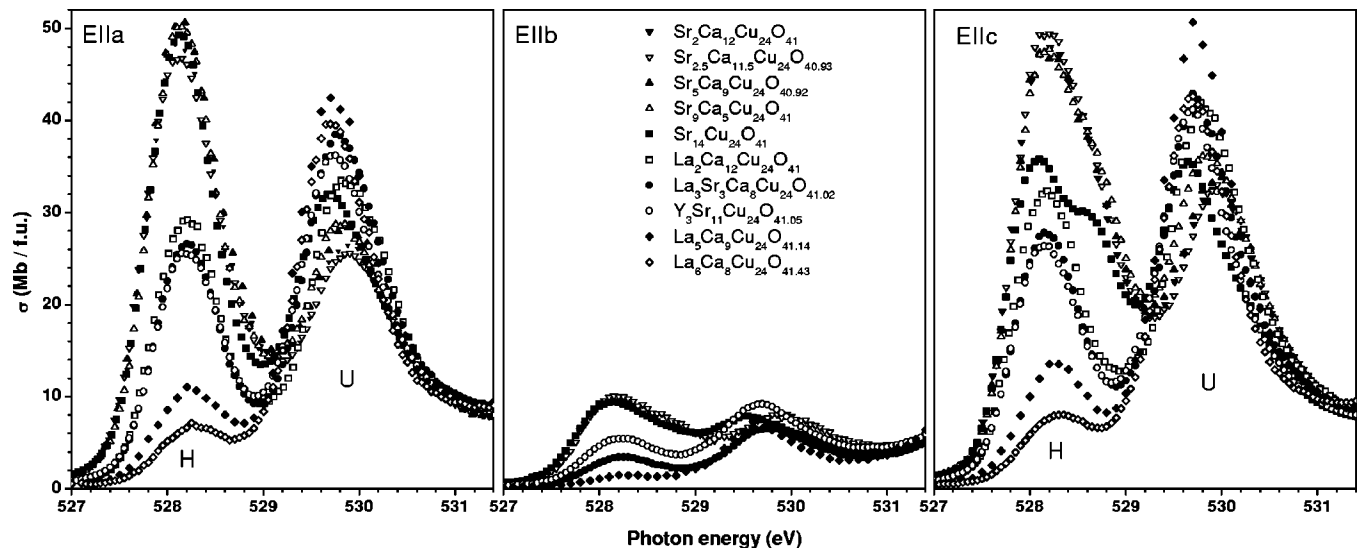


FIG. 3. Polarization-dependent O 1s NEXAFS spectra for $\text{La}_6\text{Ca}_8\text{Cu}_{24}\text{O}_{41.4}$, $\text{La}_5\text{Ca}_9\text{Cu}_{24}\text{O}_{41.4}$, $\text{La}_3\text{Sr}_5\text{Ca}_8\text{Cu}_{24}\text{O}_{41}$, $\text{Y}_3\text{Sr}_{11}\text{Cu}_{24}\text{O}_{41}$, $\text{La}_2\text{Ca}_{12}\text{Cu}_{24}\text{O}_{41}$, $\text{Sr}_{14}\text{Cu}_{24}\text{O}_{41}$, $\text{Sr}_9\text{Ca}_5\text{Cu}_{24}\text{O}_{41}$, $\text{Sr}_5\text{Ca}_9\text{Cu}_{24}\text{O}_{41}$, and $\text{Sr}_2\text{Ca}_{12}\text{Cu}_{24}\text{O}_{41}$ for polarizations $\mathbf{E}\parallel a$, $\mathbf{E}\parallel b$, and $\mathbf{E}\parallel c$. The first feature (H) represents holes at the O sites, and the second one (U) the upper Hubbard band. For $\mathbf{E}\parallel b$, only a subset of spectra is depicted to retain clarity.

trating first on the “planar” $\mathbf{E}\parallel a,c$ spectra one observes considerable spectral weight near threshold. The first feature above threshold, around 528 eV and called H in the spectra, appears near the O 1s binding energy as determined by x-ray photoemission spectroscopy (not shown). Feature H , therefore, represents hole states; its spectral weight is related to the number of holes per unit cell. Analogous to the situation for HTSC materials, a second maximum is observed in the spectra which represents the upper Hubbard band (UHB) and is denoted by U . It appears in the O 1s spectra due to the Cu $3d-0\ 2p$ hybridization, the strength of which is described by the hopping integral t_{pd} . The spectral weight of feature H is smallest for $\text{La}_6\text{Ca}_8\text{Cu}_{24}\text{O}_{41.43}$ and grows with the Sr and/or Ca content, i.e., with the number of doped holes. At the same time, the spectral weight of feature U is seen to decrease. Particularly noteworthy is that the NEXAFS spectra of $\text{Y}_3\text{Sr}_{11}\text{Cu}_{24}\text{O}_{41}$ and $\text{La}_3\text{Sr}_3\text{Ca}_8\text{Cu}_{24}\text{O}_{41}$, both doped with three holes per formula unit, are identical within the experimental precision despite their very different Ca content; furthermore, they show equivalent spectral weight in H for $\mathbf{E}\parallel a$ and $\mathbf{E}\parallel c$. While for these two compounds, moreover, feature H is almost symmetric in energy (and nearly Gaussian shaped), one finds for the fully doped samples $\text{Sr}_{14-x}\text{Ca}_x\text{Cu}_{24}\text{O}_{41}$ a pronounced, shoulderlike asymmetry of H towards higher energy. An immediate conclusion that could be drawn from observing that these symmetries of H are present at low doping levels but absent at full doping is that for low doping (up to four holes per f.u.) all holes reside on the chain sites: only there spectral weight for $\mathbf{E}\parallel a$ and $\mathbf{E}\parallel c$ is naturally the same as both orientations measure equal projections of the *same* O $2p$ orbitals (cf. Fig. 1). This is in agreement with previous work (cf. Refs. 6 and 7). For $\mathbf{E}\parallel b$, a similar double-peak structure in the energy range shown is observed; the corresponding spectral weights are, however, smaller by an order of magnitude compared to the total in-plane weight for $\mathbf{E}\parallel a,c$. This is a nice illustration of the predominantly planar character of the electronic structure near E_F for both the chain and the ladder units.

These qualitative observations can be put on a somewhat firmer footing by a more refined data analysis based on the following ideas: Systematic changes in H and U upon hole doping and upon Ca substitution, like the developing asymmetries in H described above, can clearly be observed in Fig. 3, although individual O $2p$ contributions are not well separated from each other. With the present study, on the other hand, a large number of spectra for different compositions are available, and a promising way to extract as much site-specific information as possible is to perform a least-squares fit to *all* measured spectra *simultaneously*. With the assumption that for all compositions the individual, site-specific spectral distributions are identical in shape, and that only their amplitudes and energy positions may change with composition, one can even construct these spectral distributions corresponding to various O orbitals in the fitting procedure, and thus avoid introducing artifacts through a possibly imperfect choice of spectral shapes for the fitting functions. Of course, the spectral weight and energy shifts for each composition are also obtained in the same fit. The spectra for $\text{La}_6\text{Ca}_8\text{Cu}_{24}\text{O}_{41.43}$ and $\text{La}_5\text{Ca}_9\text{Cu}_{24}\text{O}_{41.14}$ were not included in the fitting procedure for construction of the spectral distributions since their strong off-stoichiometry might possibly

lead to artifacts in the results. Their partial weight, however, was calculated as well using the distributions determined from all the other spectra.

In practice one is, of course, limited in the number of spectral distributions that can reasonably be constructed in the fitting procedure; it must be much smaller than the number of independent spectra measured (generally the two in-plane spectra per sample are used). With two distributions each to fit H and U for each polarization the resulting spectral distributions for $\mathbf{E}\parallel a$ and $\mathbf{E}\parallel c$ turn out to be almost identical, allowing the use of the same distributions for both polarizations. Unlike the situation for H , where two distributions are *required* to properly approximate the experimental curve⁸ and its doping dependence, a decomposition of U into two parts is far less justified: the improvement in rms deviation is only marginal, and the variation of relative intensities does not exhibit systematic dependence on doping. It is thus possible to determine only three spectral weights: $H1$, $H2$, and U . The energies of peaks $H1$ and $H2$ associated with the doped holes remain constant to within 30 meV and are well within the limits of our energy calibration (<100 meV); such slight energy shifts could be due to changes in the O 1s binding energy. In the case of U , a single fitting function had to be used (as mentioned above) despite U being a composed feature, and the slightly larger shifts (<200 meV) observed for this fitting function may result from this simplification. The spectral weights fitted are discussed in the following.

In Fig. 4 NEXAFS spectra with these three fitted partial distributions are shown for $\text{Y}_3\text{Sr}_{11}\text{Cu}_{24}\text{O}_{41}$, $\text{Sr}_{14}\text{Cu}_{24}\text{O}_{41}$, and $\text{Sr}_2\text{Ca}_{12}\text{Cu}_{24}\text{O}_{41}$ for $\mathbf{E}\parallel a$ and $\mathbf{E}\parallel c$ as representative examples for the full data set. The partial weights extracted from such fits, corresponding to hole counts and the weight in the UHB, as well as their evolution as a function of the hole count as derived from volumetry and of the Ca substitution level are shown in Fig. 5: part (a) depicts the individual contributions $H1$ and $H2$ for $\mathbf{E}\parallel a$ and $\mathbf{E}\parallel c$, while part (b) plots the total weight of H (i.e., $H1 + H2$ summed over both in-plane polarizations) and the analogously determined total weight for U . The left-hand side of both panels in Fig. 5 corresponds to increasing total doping levels, while the right-hand side depicts $\text{Sr}_{14-x}\text{Ca}_x\text{Cu}_{24}\text{O}_{41}$ samples fully doped with six holes.

Concentrating first on part (b) in Fig. 5, we observe the total weight H to increase linearly with doping level as derived by the chemical analysis up to the fully doped compound $\text{Sr}_{14}\text{Cu}_{24}\text{O}_{41}$. At the same time, the weight U of the UHB decreases. This trend in U is seen to continue smoothly into the range of the Ca-substituted compounds—unlike the behavior of H , which stays constant for Ca contents greater than 4. Turning now to the polarization-dependent decomposition of H into $H1$ and $H2$ [Fig. 5(a)], it is evident that up to and including the compound $\text{La}_2\text{Ca}_{12}\text{Cu}_{24}\text{O}_{41}$ with its four doped holes, almost all the weight is found in the lower-energy part $H1$, and that it is almost the same for $\mathbf{E}\parallel a$ and $\mathbf{E}\parallel c$ absorption. The straight line shown describes this behavior for $H1$ well. ($H2$ remains below 2 Mb eV per formula unit, and this value may be taken as the “threshold of significance” for the spectral decomposition procedure described above; the absence of significant spectral weight other than that for $H1$ again illustrates that the latter repre-

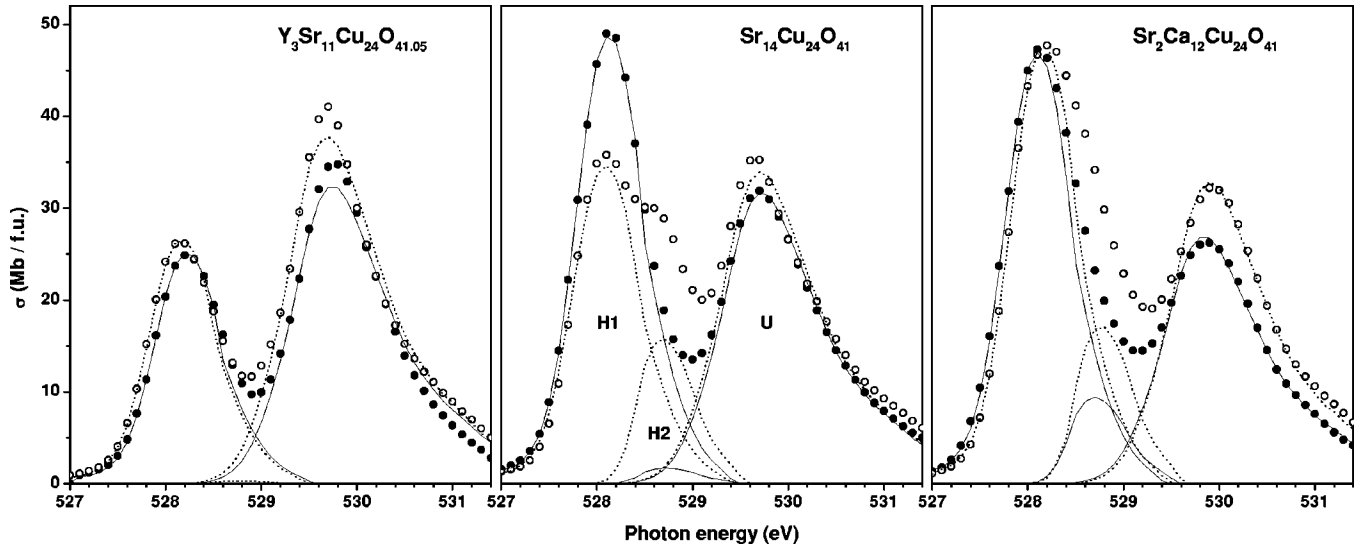


FIG. 4. NEXAFS spectra of $\text{Y}_3\text{Sr}_{11}\text{Cu}_{24}\text{O}_{41}$, $\text{Sr}_{14}\text{Cu}_{24}\text{O}_{41}$, and $\text{Sr}_2\text{Ca}_{12}\text{Cu}_{24}\text{O}_{41}$ for $\mathbf{E}\parallel a$ (filled symbols) and $\mathbf{E}\parallel c$ (open symbols) along with the fitted partial distributions corresponding to holes ($H1$ and $H2$) and to the upper Hubbard band (U); see text. Spectral weight above 531 eV corresponding to states other than H and U was subtracted (Ref. 32).

sents doped holes in the chain.) For $\text{Sr}_{14}\text{Cu}_{24}\text{O}_{41}$, the situation changes considerably: $H1$ for $\mathbf{E}\parallel c$ lies substantially below its $\mathbf{E}\parallel a$ counterpart (which itself remains close to the straight line extrapolated from the lower doping levels), and for the first time, there is a significant contribution from $H2$, amounting to almost 1/3 of $H1$. The corresponding $H2$ for $\mathbf{E}\parallel a$, on the other hand, is still almost zero. In the total weight [Fig. 5(b)] the decrease of $H1$ is thus compensated for. For the partially Ca-substituted compound $\text{Sr}_9\text{Ca}_5\text{Cu}_{24}\text{O}_{41}$, $H1$ for $\mathbf{E}\parallel c$ is substantially larger than for $\text{Sr}_{14}\text{Cu}_{24}\text{O}_{41}$; further increasing the Ca content then leaves both $H1$ parts almost constant, similar to the behavior of the total H . $H2$ for $\mathbf{E}\parallel c$, on the other hand, remains constant for all Ca-substitution levels, while $H2$ for $\mathbf{E}\parallel a$ exhibits a slight increase over the whole range of Ca fractions,³³ until it reaches, for $\text{Sr}_2\text{Ca}_{12}\text{Cu}_{24}\text{O}_{41}$, about 1/6 of the value for $H1$.

III. INTERPRETATION AND DISCUSSION

The observation that for $\text{La}_3\text{Sr}_3\text{Ca}_8\text{Cu}_{24}\text{O}_{41}$, $\text{Y}_3\text{Sr}_{11}\text{Cu}_{24}\text{O}_{41}$, and $\text{La}_2\text{Ca}_{12}\text{Cu}_{24}\text{O}_{41}$, H consists of only one component, $H1$, which is furthermore almost symmetric within the a,c plane, is readily understood if the holes at these doping levels almost exclusively occupy sites in the chains. In the fully doped compound $\text{Sr}_{14}\text{Cu}_{24}\text{O}_{41}$, however, this symmetry is obviously broken (see above). Most significant is the appearance of $H2$, which for $\mathbf{E}\parallel c$ exhibits considerable weight but for $\mathbf{E}\parallel a$ still barely exceeds the “threshold of significance.” These observations unambiguously show that $H2$ must be the spectral weight corresponding to holes on the O(1) sites of the legs: only there do O $2p_\sigma$ orbitals exist which can contribute strongly to the $\mathbf{E}\parallel c$ weight while not at the same time leading to a similarly strong $\mathbf{E}\parallel a$ weight; cf. Fig. 1. Energetically, $H2$ is observed at ≈ 0.6 eV above $H1$, consistent with the interpretation that the corresponding holes reside on O sites in different atomic environments. On the other hand, the $\mathbf{E}\parallel a$ from the O(1) leg site should appear at an energy very similar to that for the

$\mathbf{E}\parallel c$ contributions, as both involve the same core level energy. While possible holes on the rung O(2) sites would appear for $\mathbf{E}\parallel a$ only it is not so clear, however, where in energy this contribution would show up in the spectrum.

In the following, we present a more detailed picture of the hole distribution and the upper Hubbard bands, trying to account for all observations made so far, and check it against

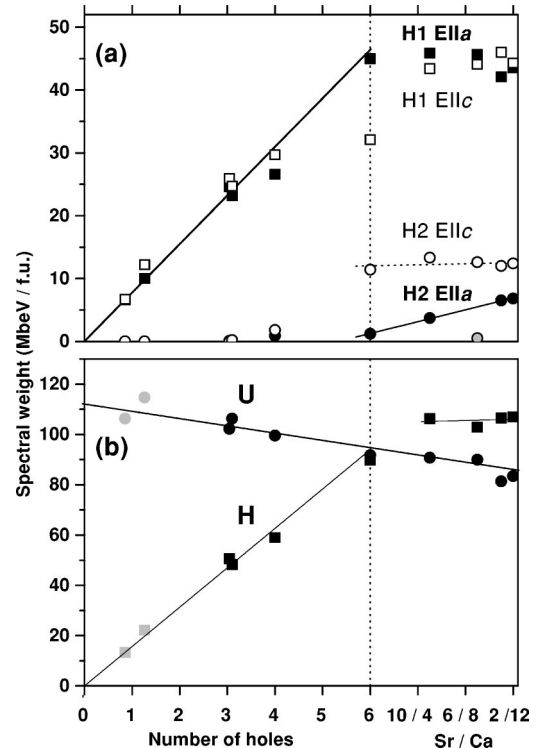


FIG. 5. Evolution of partial in-plane weights $H1$, $H2$ of holes [panel (a)], and total spectral weight of H and U [panel (b)] for $(\text{Sr,Ca,Y,La})_{14}\text{Cu}_{24}\text{O}_{41}$ compounds resulting from the least-squares fit of three distributions to all spectra measured. Gray symbols correspond to data with less experimental significance, e.g., if some La segregation occurs (see text). Lines are guides to the eye.

further experimental results as we proceed.

(i) As discussed above, $H1$ is ascribed to the spectral weight of holes residing on the chain $O(c)$ sites, giving a highly symmetric in-plane contribution in NEXAFS. The asymmetry between $\mathbf{E}\parallel a$ and $\mathbf{E}\parallel c$ at high doping levels, most prominently displayed by $\text{Sr}_{14}\text{Cu}_{24}\text{O}_{41}$, may have its origin in certain lattice distortions of the chains along c , as observed by x-ray diffraction¹⁶ for temperatures below room temperature. These distortions appear simultaneously with spin dimerization and lead to deviations from the otherwise 90° Cu-O-Cu bond symmetry. NEXAFS as a local probe is still sensitive to the asymmetry³⁴ induced in this way to the hole distribution of the chain, even though at room temperature long-range order is already lost.

(ii) $H2$ is observed experimentally for $\mathbf{E}\parallel c$ and to a smaller extent for $\mathbf{E}\parallel a$ as well and is thus ascribed mainly to the spectral weight of holes residing on the leg $O(1)$ sites of the ladder. Increasing the Ca content x for the fully doped compounds $\text{Sr}_{14-x}\text{Ca}_x\text{Cu}_{24}\text{O}_{41}$ [right-hand side of Fig. 5(b)] does not change $H2$ appreciably for $\mathbf{E}\parallel c$, indicating that no more holes are transferred to the $O(1)$ $2p_z$ orbitals; the increase of $H2$ observed for $\mathbf{E}\parallel a$ points to a small but increasing number of holes that are transferred to ladder orbitals oriented along the a axis. The data do not allow one to decide unambiguously if this transfer takes place to leg $O(1)$ sites and/or rung $O(2)$ sites.

(iii) U consists of the spectral weight of both the chain UHB and the ladder UHB, and the fact that the fitting procedure described above was not able to separate these two contributions may indicate that the energetic positions and spectral distributions are too similar for all compositions. The in-plane Cu-O coordination and the Cu-O bond lengths in both the chain and the ladder units are almost identical and hence t_{pd} will be to a good approximation the same for chains and ladders. In the undoped compound $\text{La}_6\text{Ca}_8\text{Cu}_{24}\text{O}_{41.4}$ there are 10 Cu $3d$ holes per f.u. in the chain and 14 Cu $3d$ holes per f.u. in the ladder unit. Hence one can expect the respective spectral weights in the UHB as observed in $O 1s$ NEXAFS to be distributed accordingly: about 47:65 Mb eV for the chain vs the ladder UHB. Hole doping of the chain by about 5 holes for $\text{Sr}_{14}\text{Cu}_{24}\text{O}_{41}$ (see above) results in a formal Cu(c) valence of +2.5, which in most cuprates would result in an almost complete transfer of spectral weight from the UHB to the hole states H . Experimentally, we observe a reduction in the total U by <20 Mb eV when going from $n_h=0$ to $n_h=6$ in the left-hand part of Fig. 5(b). Doping of just a single hole per f.u. into the ladder unit of $\text{Sr}_{14}\text{Cu}_{24}\text{O}_{41}$ will raise the formal Cu(l) valence only to +2.07, and the associated reduction of the ladder UHB will be far smaller than for the chain unit with Cu(c)^{+2.50}. We may thus assign the full reduction observed for U to the chain UHB and find that for $\text{Sr}_{14}\text{Cu}_{24}\text{O}_{41}$, at most 45% of the spectral weight for the fully developed chain UHB is transferred to H . This is considerably less than observed for doped CuO_2 planes in high- T_c cuprates, and even for the closely related doped chain structure of $\text{Sr}_{0.73}\text{CuO}_2$ with a formal Cu valence of 2.54 the spectral weight of the UHB has almost vanished.³¹ One does find for edge-sharing chains like the ones in the present study a Cu-O-Cu hopping that is strongly hampered as it is not only governed by t_{pd} but is mediated by two different in-plane O

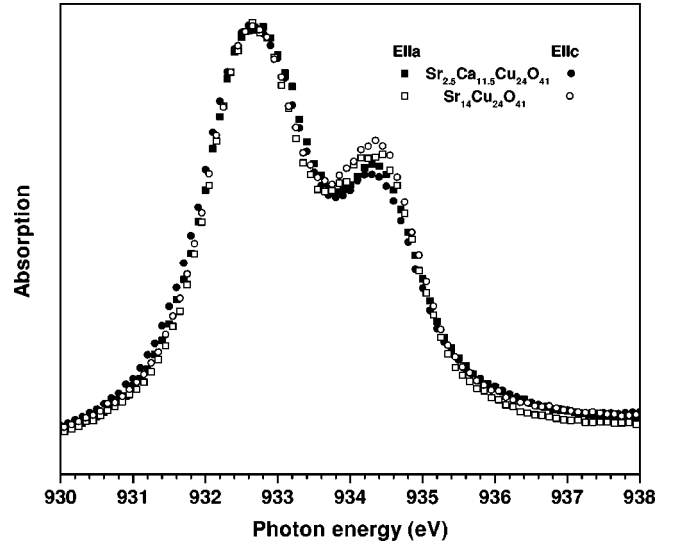


FIG. 6. Polarization-dependent Cu $2p_{3/2}$ NEXAFS for $\text{Sr}_{14}\text{Cu}_{24}\text{O}_{41}$ and $\text{Sr}_{2.5}\text{Ca}_{11.5}\text{Cu}_{24}\text{O}_{41}$, taken in fluorescence yield mode but with no self-absorption correction applied (see text). All spectra are normalized to equal amplitude in the “white line” around 932.5 eV. The ligand-hole peak at about 934 eV provides evidence that t_{pd} is reduced for high Ca substitution for Sr.

$2p$ orbitals that are mutually orthogonal,^{35,36} which should result in a relatively slow transfer of spectral weight from the UHB to H upon hole doping.³⁷ The difference to $\text{Sr}_{0.73}\text{CuO}_2$ which consists of edge-sharing chains as well may be that there the Cu-O-Cu bond angles are in fact not as close to 90° as in the chains of the $\text{Sr}_{14}\text{Cu}_{24}\text{O}_{41}$ family.

(iv) The spectral weight for $\mathbf{E}\parallel b$ is too small to be interpreted individually, especially against the backdrop of the large contributions for $\mathbf{E}\parallel a, c$. Thus, even small factors like the about 97% degree of linear polarization or possible small misalignments, both mixing small fractions of the planar spectral weight to the $\mathbf{E}\parallel b$ spectra, may affect the results for $\mathbf{E}\parallel b$ and their relationship to the hole counts for the ladder sites which are also small. It may still be allowed to note that the spectral weight in the hole peak for $\mathbf{E}\parallel b$ tracks, in general, the nominal hole doping level; yet one also notes that for $\text{Sr}_{14}\text{Cu}_{24}\text{O}_{41}$ and $\text{Sr}_2\text{Ca}_{12}\text{Cu}_{24}\text{O}_{41}$, the $\mathbf{E}\parallel b$ component is unusually high.

(v) The observation made in the previous section that the total spectral weight H , which in turn is dominated by the chain $H1$, is significantly larger for the Ca-substituted compound $\text{Sr}_9\text{Ca}_5\text{Cu}_{24}\text{O}_{41}$ than for $\text{Sr}_{14}\text{Cu}_{24}\text{O}_{41}$ is highly intriguing: stoichiometry requires the total number of holes to be the same. A possible solution for this puzzle is suggested by looking at the Cu $2p_{3/2}$ NEXAFS spectra for $\text{Sr}_{14}\text{Cu}_{24}\text{O}_{41}$ and $\text{Sr}_{2.5}\text{Ca}_{11.5}\text{Cu}_{24}\text{O}_{41}$ shown in Fig. 6. They are recorded in fluorescence yield mode, but as self-absorption effects are exceedingly strong at this edge, corrections like the ones applied to the $O 1s$ edge (see above) are problematic here and thus were not performed. Total electron yield spectra, on the other hand, would not be reliable as the sample surfaces could not be cleaved *in situ*. As the large Hubbard correlation energy enforces a Cu $3d^9$ ground state with one intrinsic hole per Cu site, it is still possible to at least qualitatively compare different samples by normalizing the amplitudes of the excitonic peak (or “white line”) around 932.5 eV. Ob-

serving a significantly *lower* ligand-hole peak at about 934 eV for the highly Ca-substituted compound—while the corresponding weight $H1$ for O $1s$ NEXAFS is clearly *higher*—may thus be interpreted as a signature for a reduced t_{pd} hopping parameter in the chains, with the immediate consequence that the doped holes have increased O $2p$ character for heavy Ca substitution. This apparent decrease in the chain t_{pd} is likely to be induced by strong distortions of the chain⁵ on incorporation of much smaller Ca atoms, leading to highly inequivalent O sites in the chain with Cu(*c*)-O(*c*) distances varying (for Sr_{0.4}Ca_{13.6}Cu₂₄O₄₁) from 1.71 Å to 2.02 Å,⁵ and presumably to a quite inhomogeneous redistribution of holes. Thus the observation of a reduced t_{pd} in NEXAFS does not stand in contrast to the structural observation of a reduced average Cu(*c*)-O(*c*) bond length but may be taken as an indication that the doped holes in the chain may be located preferably on O sites associated with a smaller effective t_{pd} .

(vi) The fact that the spectral weight of U for the fully doped compounds Sr_{14-x}Ca_xCu₂₄O₄₁ seems to decrease with increasing x is qualitatively consistent with the slight increase observed for $H2$ in this substitutional regime: if holes are redistributed from chain sites to ladder sites, the “slow” transfer of spectral weight between H and the UHB for the chains [see (iii) above] would lead to a concurrent increase in the chain UHB that is smaller than and thus overcompensated by the decrease in the ladder UHB. The slope of U appears larger than that of $H2$ and thus at first glance suggests possible inconsistencies. It should be noted, however, that upon Ca substitution the chain t_{pd} is reduced [see (v) above] and lattice distortions increase, presumably resulting in deviations from the 90° Cu-O-Cu bond geometry. Both effects directly lead to a reduction of the spectral weight of the chain UHB in O $1s$ NEXAFS and help to explain the decrease in U observed in the right-hand part of Fig. 5(b).

It is interesting to estimate the absolute hole counts $n_{i,E}$ related to the various O orbitals, where i denotes spectral weight corresponding to $H1$ or $H2$, and E denotes the polarization. For each sample, the total spectral weight of H , summed over the in-plane polarizations, is directly equated to the corresponding total hole count as determined by the precision chemical analysis described above. The individual contributions $n_{i,E}$ directly follow from this “normalization.” In this way, the problems associated with possible changes in parameters like t_{pd} , for which an indication has been presented in (v) above, are reduced in their effect on the individual hole occupation numbers determined. The results are shown in Fig. 7. The hole count most obviously associated with the ladders, $n_{2,a} + n_{2,c}$, increases slightly from 0.8 holes for Sr₁₄Cu₂₄O₄₁ to 1.1 holes for Sr₂Ca₁₂Cu₂₄O₄₁; considering the individual contributions one observes that the increase is due to $n_{2,a}$ only while $n_{2,c}$ stays virtually constant, in effect rendering the hole distribution in ladders more two dimensional (2D) for the heavily Ca-substituted compounds.

This partial hole occupation at the ladder sites for fully doped compounds with high Ca content remains considerably smaller than the up to 2.8 holes found in optical measurements.¹¹ The interpretation of the optical data rests on assuming zero mobility for holes on the chains, allowing one to distinguish between holes on the chains (localized) and holes on the ladders (mobile). This may be less valid if

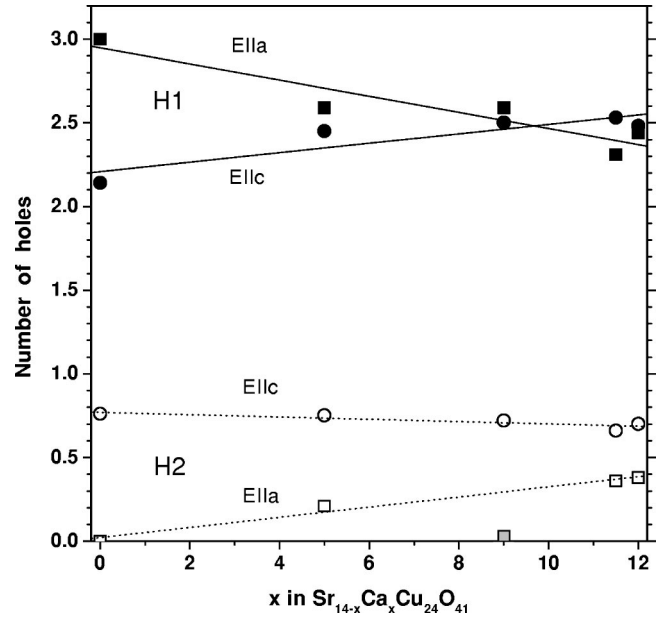


FIG. 7. Hole count per formula unit as derived from renormalized spectral weights in NEXAFS (see text) for Sr_{14-x}Ca_xCu₂₄O₄₁. Shown are contributions from O $2p$ orbitals oriented along the a and c axes in chain and ladder units.

heavy Ca substitution leads to mobility in the chain as well, and the hole count for the ladders might thus be overestimated to some extent, but even in this case the difference between the optical and NEXAFS results appears too large. A point raised in Ref. 12 concerns the role of an effective mass greater than one which would reduce the apparent ladder hole count deduced from the optical data; however, the assumption of $n_{chain}=5$ and $n_{ladder}=1$ made in Ref. 11 to “normalize” their data already takes care of this. On the other hand, conclusions drawn from NEXAFS suffer to some extent from changes in parameters like t_{pd} as pointed out above. A further effect could be that the holes on the rung O(2) sites might appear in NEXAFS at about the same energy as holes on the chain O(*c*) sites and thus would, in the evaluation used here, be counted not as a ladder contribution but instead as a chain contribution. If present at all, however, this effect is also expected to be small. The differing results of optical and x-ray determinations of the hole count are thus noted but remain unexplained at this time.

A further remark should be made on the fact that in the original work reporting on superconductivity in these ladder compounds,³ the very compound studied (Sr_{0.4}Ca_{13.6}Cu₂₄O_{41.84}) exhibited an excess oxygen content δ amounting to as much as 0.84. Although it is difficult to estimate the effect of up to 1.7 extra holes, it seems clear that such additional O atoms may lead to further substantial deformations in the crystal structure, and one could thus speculate that the hole concentration on the ladder sites may be increased considerably by the extra oxygen. Excess oxygen, on the other hand, may not even be necessary for superconductivity, as later reports^{20,38} are much less specific on excess oxygen content, and we note that crystals from the same growth rods as our Sr_{2.5}Ca_{11.5}Cu₂₄O_{40.93} and Sr₂Ca₁₂Cu₂₄O₄₁ samples do exhibit superconductivity under high pressure. It may thus well be just the increased “2D” character of the electronic structure of the ladders, detected in NEXAFS as

the increasingly similar $H2$ weight along a and c , as well as the increased number of ‘‘pseudoapical’’ O sites induced by the distortions, that in the end work together to support superconductivity in the highly Ca-substituted compounds under high pressure.

IV. CONCLUSION

Polarization-dependent NEXAFS has been performed on a large number of single-crystalline members of the $\text{Sr}_{14}\text{Cu}_{24}\text{O}_{41}$ family of layered compounds containing two-leg Cu_2O_3 ladders and CuO_2 chains. Studying different substitution levels of Y or La for Sr to change the total number of holes has shown in a direct and straightforward manner that for low and intermediate hole counts, all holes reside on the chain sites, and that this is independent of whether a further fraction of Sr is replaced by isoelectronic Ca as well. For the fully doped compound $\text{Sr}_{14}\text{Cu}_{24}\text{O}_{41}$, on the other hand, approximately one hole per formula unit is observed on the ladder unit, specifically in O $2p$ orbitals oriented

along the c axis on the legs. Studying the fully doped substitution series $\text{Sr}_{14-x}\text{Ca}_x\text{Cu}_{24}\text{O}_{41}$, we find the total hole count in the ladders to increase only marginally; however, a larger fraction of O $2p$ orbitals oriented along the a axis (on the legs and possibly on the rungs of the ladder) is now contributing to the spectral weight.

ACKNOWLEDGMENTS

We greatly appreciate generous and valuable experimental help by J.-H. Park, S. L. Hulbert, P. Schweiss, T. Ivanova, E. Sohmen, D.-H. Lu, and C. S. Gopinath. For illuminating discussions we are grateful to S.-L. Drechsler and M. Knupfer. Research was carried out in part at the National Synchrotron Light Source, Brookhaven National Laboratory, which is supported by the U.S. Department of Energy, Division of Material Sciences and Division of Chemical Sciences, under Contract No. DE-AC02-98CH10886. V.C. was supported by the Office of Naval Research.

*Present address: Robert Bosch GmbH, Center of Research and Development, P.O. Box 1342, D-72762 Reutlingen, Germany.

[†]Present address: Experimental Facilities Division, Argonne National Laboratory, Argonne, IL 60439.

¹K. Totsuka and M. Suzuki, *J. Phys.: Condens. Matter* **7**, 6079 (1995); N. Katoh and M. Imada, *J. Phys. Soc. Jpn.* **64**, 1437 (1995); E. Dagotto and T. M. Rice, *Science* **271**, 618 (1996); C. Kim, Z.-X. Shen, N. Motoyama, H. Eisaki, S. Uchida, and T. Tohyama, *Phys. Rev. B* **56**, 15 589 (1997).

²T. M. Rice, S. Gopalan, and M. Sigrist, *Europhys. Lett.* **23**, 445 (1993).

³M. Uehara, T. Nagata, J. Akimitsu, H. Takahashi, N. Mōri, and K. Kinoshita, *J. Phys. Soc. Jpn.* **65**, 2764 (1996).

⁴E. M. McCarron III, M. A. Subramanian, J. R. Calabrese, and R. L. Harlow, *Mater. Res. Bull.* **23**, 1355 (1988); K. Kato, *Acta Crystallogr., Sect. B: Struct. Sci.* **46**, 39 (1990); K. Ukei, T. Shishido, and T. Fukuda, *ibid.* **50**, 42 (1994); K. Kato, E. Takyama-Muromachi, K. Kosuda, and Y. Uchida, *ibid.* **44**, 1881 (1988).

⁵T. Siegrist, L. F. Schneemeyer, S. A. Sunshine, J. V. Wasczak, and R. S. Roth, *Mater. Res. Bull.* **23**, 1429 (1988); T. Ohta, F. Izumi, M. Onoda, M. Isobe, E. Takayama-Muromachi, and A. W. Hewat, *J. Phys. Soc. Jpn.* **66**, 3107 (1997).

⁶M. Kato, K. Shiotani, and Y. Koike, *Physica C* **258**, 284 (1996); M. Isobe and E. Takayama-Muromachi, *J. Phys. Soc. Jpn.* **67**, 3119 (1998).

⁷S. A. Carter, B. Batlogg, R. J. Cava, J. J. Krajewski, W. F. Peck, Jr., and T. M. Rice, *Phys. Rev. Lett.* **77**, 1378 (1996).

⁸The energy shift between $H1$ and $H2$ was treated as a fit parameter as well but was assumed to be the same for all spectra.

⁹M. Matsuda, K. Katsumata, H. Eisaki, N. Motoyama, S. Uchida, S. M. Shapiro, and G. Shirane, *Phys. Rev. B* **54**, 12 199 (1996).

¹⁰R. S. Eccleston, M. Uehara, J. Akimitsu, H. Eisaki, N. Motoyama, and S. Uchida, *Phys. Rev. Lett.* **81**, 1702 (1998); L. P. Regnault, J. P. Boucher, H. Moudden, J. E. Lorenzo, A. Hiess, U. Ammerahl, G. Dhalenne, and A. Revcolevschi, *Phys. Rev. B* **59**, 1055 (1999); M. Matsuda, T. Yoshihama, K. Kakurai, and G. Shirane, *ibid.* **59**, 1060 (1999).

¹¹T. Osafune, N. Motoyama, H. Eisaki, and S. Uchida, *Phys. Rev. Lett.* **78**, 1980 (1997).

¹²B. Ruzicka, L. Degiorgi, U. Ammerahl, G. Dhalenne, and A. Revcolevschi, *Eur. Phys. J. B* **6**, 301 (1998); B. Ruzicka, L. Degiorgi, G. I. Meijer, J. Karpinski, U. Ammerahl, G. Dhalenne, and A. Revcolevschi, *Physica C* **317-318**, 282 (1999).

¹³K. Magishi, S. Matsumoto, Y. Kitaoka, K. Ishida, K. Asayama, M. Uehara, T. Nagata, and J. Akimitsu, *Phys. Rev. B* **57**, 11 533 (1998).

¹⁴M. Takigawa, N. Motoyama, H. Eisaki, and S. Uchida, *Phys. Rev. B* **57**, 1124 (1998).

¹⁵S. Ohsugi, K. Magishi, S. Matsumoto, Y. Kitaoka, T. Nagata, and J. Akimitsu, *Phys. Rev. Lett.* **82**, 4715 (1999).

¹⁶D. E. Cox, T. Iglesias, K. Hirota, G. Shirane, M. Matsuda, N. Motoyama, H. Eisaki, and S. Uchida, *Phys. Rev. B* **57**, 10 750 (1998).

¹⁷S. Tsuji, K. Kumagai, M. Kato, and Y. Koike, *J. Phys. Soc. Jpn.* **65**, 3474 (1996).

¹⁸S. Katano, T. Nagata, J. Akimitsu, M. Nishi, and K. Kakurai, *Phys. Rev. Lett.* **82**, 636 (1999).

¹⁹S. Pachot, P. Bordet, R. J. Cava, C. Chailout, C. Darie, M. Hanfland, M. Marezio, and H. Takagi, *Phys. Rev. B* **59**, 12 048 (1999).

²⁰M. Isobe, T. Ohta, M. Onoda, F. Izumi, S. Nakano, J. Q. Li, Y. Matsui, E. Takayama-Muromachi, T. Matsumoto, and H. Hayakawa, *Phys. Rev. B* **57**, 613 (1998).

²¹T. F. A. Müller, V. Anisimov, T. M. Rice, I. Dasgupta, and T. Saha-Dasgupta, *Phys. Rev. B* **57**, R12 655 (1998).

²²Y. Mizuno, T. Tohyama, and S. Maekawa, *J. Phys. Soc. Jpn.* **66**, 937 (1997); K. Magishi, S. Matsumoto, Y. Kitaoka, K. Ishida, K. Asayama, M. Uehara, T. Nagata, and J. Akimitsu, *Phys. Rev. B* **57**, 11 533 (1998); M. V. Abrashev, C. Thomsen, and M. Surtchev, *Physica C* **280**, 297 (1997).

²³N. Motoyama, T. Osafune, T. Kakeshita, H. Eisaki, and S. Uchida, *Phys. Rev. B* **55**, R3386 (1997); U. Ammerahl, G. Dhalenne, A. Revcolevschi, J. Berthon, H. Moudden, *J. Cryst. Growth* **193**, 55 (1998).

²⁴U. Ammerahl and A. Revcolevschi, *J. Cryst. Growth* **197**, 825 (1999).

- ²⁵K. Conder, S. Rusiecki, and E. Kaldis, *Mater. Res. Bull.* **24**, 581 (1989).
- ²⁶L. Tröger, D. Arvanitis, K. Baberschke, H. Michaelis, U. Grimm, and E. Zschech, *Phys. Rev. B* **46**, 3283 (1992); S. Eisebitt, T. Böske, J.-E. Rubensson, and W. Eberhardt, *ibid.* **47**, 14 103 (1993).
- ²⁷J. J. Yeh and I. Lindau, *At. Data Nucl. Data Tables* **32**, 1 (1985).
- ²⁸M. Knupfer (private communication).
- ²⁹F. Sapiña, J. Rodríguez-Carvajal, M. J. Sanchis, R. Ibáñez, A. Beltrán, and D. Beltrán, *Solid State Commun.* **74**, 779 (1990).
- ³⁰R. Neudert, H. Rosner, S.-L. Drechsler, M. Kielwein, M. Sing, Z. Hu, M. Knupfer, M. S. Golden, J. Fink, N. Nücker, M. Merz, S. Schuppler, N. Motoyama, H. Eisaki, S. Uchida, M. Domke, and G. Kaindl, *Phys. Rev. B* **60**, 13 413 (1999).
- ³¹R. Neudert, M. Sing, M. Kielwein, Z. Hu, M. Knupfer, M. S. Golden, J. Fink, J. Karpinski, N. Motoyama, H. Eisaki, S. Uchida, G. Kaindl, C. Hellwig, and Ch. Jung (unpublished).
- ³²To obtain spectra for the fitting procedure that consist solely of H and U , the higher-energy part of each spectrum was removed by approximating it, for the region of U and up to 534 eV, by a Gaussian which was then subtracted.
- ³³For $\text{Sr}_5\text{Ca}_9\text{Cu}_{24}\text{O}_{41}$, $H2$ for $\mathbf{E}\parallel a$ is less significant due to experimental difficulties: possible inhomogeneities and a slight misorientation will affect this contribution the most as it is the smallest. In Figs. 5(b) and 7 the respective data point is thus depicted in a gray shade.
- ³⁴The asymmetric NEXAFS results for $\text{Sr}_{14}\text{Cu}_{24}\text{O}_{41}$ could also be viewed as a signature for a [spin-density-wave- (SDW-) or CDW-derived] gap, and a very rough estimate of its size could be obtained like this: a peak *area* in NEXAFS near threshold corresponds to the number of states (doped holes), and thus the peak *amplitude* right above threshold gives an approximation for the density of states near E_F . From Fig. 3 one reads off a total amplitude of ≈ 85 Mb for $H1$, and thus the a, c asymmetry of ≈ 12 Mb eV (Fig. 5) would correspond to a shift of $12/85 \approx 0.14$ eV between the a and c components of the spectral weight distributions. This value far exceeds, however, any spin gap reported for the chain (≤ 15 meV).
- ³⁵Y. Mizuno, T. Tohyama, S. Maekawa, T. Osafune, N. Motoyama, H. Eisaki, and S. Uchida, *Phys. Rev. B* **57**, 5326 (1998); S. Tornow, O. Entin-Wohlman, and A. Aharony, *ibid.* **60**, 10 206 (1999).
- ³⁶In Ref. 30, transfer integrals in the range 30–80 meV along the chains of Li_2CuO_2 are presented, which are smaller by a factor of at least 7 compared to the value (0.55 eV) for the corner-sharing chain compound Sr_2CuO_3 where Cu-O-Cu hopping is not hampered.
- ³⁷M. B. J. Meinders, H. Eskes, and G. A. Sawatzky, *Phys. Rev. B* **48**, 3916 (1993).
- ³⁸T. Nagata, M. Uehara, J. Goto, N. Komiya, J. Akimitsu, N. Motoyama, H. Eisaki, S. Uchida, H. Takahashi, T. Nakanishi, and N. Môri, *Physica C* **282-287**, 153 (1997).